

University of Groningen

## Langmuir-Blodgett films of amylose-esters and chiral azo-dyes

Schoondorp, Monique Annette

**IMPORTANT NOTE:** You are advised to consult the publisher's version (publisher's PDF) if you wish to cite from it. Please check the document version below.

*Document Version*

Publisher's PDF, also known as Version of record

*Publication date:*

1992

[Link to publication in University of Groningen/UMCG research database](#)

*Citation for published version (APA):*

Schoondorp, M. A. (1992). *Langmuir-Blodgett films of amylose-esters and chiral azo-dyes: structure and second order nonlinear optical behaviour*. s.n.

### Copyright

Other than for strictly personal use, it is not permitted to download or to forward/distribute the text or part of it without the consent of the author(s) and/or copyright holder(s), unless the work is under an open content license (like Creative Commons).

The publication may also be distributed here under the terms of Article 25fa of the Dutch Copyright Act, indicated by the "Taverne" license. More information can be found on the University of Groningen website: <https://www.rug.nl/library/open-access/self-archiving-pure/taverne-amendment>.

### Take-down policy

If you believe that this document breaches copyright please contact us providing details, and we will remove access to the work immediately and investigate your claim.

Downloaded from the University of Groningen/UMCG research database (Pure): <http://www.rug.nl/research/portal>. For technical reasons the number of authors shown on this cover page is limited to 10 maximum.

## CHAPTER 4

### *Langmuir-Blodgett films of amylose-acetate / dye mixtures.*

**Langmuir-Blodgett multilayers of mixtures of amylose-acetate and a chiral p-nitro-azobenzene dye.**

#### **SUMMARY**

*The structure of multilayers of a mixture of amylose-acetate and a chiral NLO-dye, a mono-ester of **palmitic** acid and 4-nitro-4'-[(3R)-hydroxypyrrolidine-]-azobenzene (KMES16) has been studied. The monolayers of the mixed systems, consisting of domains of the dye in a matrix of amylose-acetate, were transferred by the Langmuir-Blodgett technique onto solid substrates in the Z-type transfer **mode**. The structure of the multilayers was investigated by Fourier **Transform Infrared** spectroscopy, UV-spectroscopy and small angle X-ray **diffraction**. The aliphatic chain of the dye molecule exhibits a remarkable orientation as revealed by infrared spectroscopy. These all trans **CH<sub>2</sub>** chains are tightly packed and they have a **specific** orientation around the chain director.*

*The dye fragment of the molecule appeared to be oriented at about 30° with the **surface** normal, whereas the molecules are packed antiparallel in the lamellar crystals. From UV spectroscopy it was deduced that these crystals can be considered as H-aggregates.*

*After heating the multilayers and cooling down the IR-spectra reveal a more **well-defined** structure with lamellar crystals, which also behave like H-aggregates.*

## **INTRODUCTION**

In Chapter 3<sup>1</sup> we described the monolayer behaviour of the ester of palmitic-acid and 4-nitro-4'-[(3R)-hydroxypyrrolidine]-azobenzene and mixtures of this potentially important dye for NLO-applications with amylose-acetate. It appeared that the dye alone forms stable monolayers at temperatures below 11°C and surface pressures below 7 mN/m. Upon mixing with amylose-acetate a two dimensional heterogenous system was formed, consisting of domains of dye molecules in a matrix of amylose-acetate. UV/VIS measurements indicated that the domains can be considered as H-aggregates. These H-aggregates appeared to have a narrow absorption band in the UV/VIS spectrum which was blue shifted compared to the spectrum of the dye in chloroform.

Electron diffraction of the domains revealed a pg plane group implying that the dye molecules are packed anti parallel in the unit cell.

It was not possible to transfer monolayers of the dye alone by the Langmuir-Blodgett technique under any condition tried. However, the mixtures with amylose-acetate could be transferred by the normal dipping procedures which are also suitable for amylose-acetate as found before (Chapter 2)<sup>2</sup>.

It is obvious that the characterization of the structure is an important aspect of the study of LB-multilayer systems. Techniques like X-ray diffraction, ellipsometry and IR-spectroscopy are available for studying LB-multilayers<sup>3,4,5</sup>.

The IR absorption spectra in the transmission mode and in the reflection mode yield accurate information concerning the orientation of the molecules in the multilayer. Since the optics of the reflection spectra have been investigated extensively<sup>6,7</sup> many authors have applied this technique to ultra-thin layers<sup>8,9,10,11,12,13,14,15</sup>.

Here the structure of multilayers, formed from the monolayers studied before (Chapter 3)<sup>1</sup> is reported.

## **EXPERIMENTAL**

### **Materials**

The synthesis of the ester of palmitic acid and 4-nitro-4'-[(3R)-hydroxypyrrolidine]-azobenzene, code KMES16, with a chiral center will be reported separately<sup>16</sup>. The structure is given in the previous chapter<sup>1</sup>

### **LB-measurements**

A computer controlled Lauda filmbalance FW2 was used. Transfer experiments were carried out by a vertical dipping method after stabilization of the monolayer on the water surface (unless mentioned otherwise) at constant temperature (23°C) and pressure (7mN/m). A dipping speed of 5 mm/min was used for the up and down stroke transfer. The monolayers were transferred onto glass slides, hydrophobized by treating with 1,1,1,3,3,3 hexamethyldisilazane in chloroform 1:3 v/v at 50 °C. Substrates for IR-measurements (GIR) were prepared by argon plasma sputtering of gold (thickness 500 Å) onto glass slides with a Biorad Turbo-coater E6700. For transmission experiments ZnS substrates (2mm thick Cleartran) were used.

### **Infrared Measurements**

Infrared measurements were performed with a Bruker IFS88 FTIR spectrophotometer equipped with a MCT-A D313 detector. A germanium Brewster angle IR polarizator was used for both grazing angle reflection (GIR) and transmission experiments. GIR- spectra were recorded in 80° specular set-up with light polarized parallel to the plane of incidence and referenced against the reflection of a clean gold layer. Transmission spectra were recorded from samples on ZnS using 4 cycles of 250 scans each according to the method of Arndt<sup>14</sup>. All spectra were recorded at 4 cm<sup>-1</sup> and baseline corrected.

### **UV/visible light spectra.**

UV/visible light spectra were taken from multilayers deposited at both sides of glass slides. A Pye-Unicam SP8-200 UV/Vis spectrophotometer was used.

### **X-ray diffraction**

X-ray measurements were performed with a PW 1830 generator and PW 1820 diffractometer with a monochromator in the diffracted beam. Chrome was used as radiation source. The multilayers were deposited on glass.

## **RESULTS AND DISCUSSIONS**

### **LB-multilayers**

Multilayers on different substrates were prepared from monolayers of 70 (mol%) AAC and 30 (mol%) KMES16. Multilayers were built up by a Z-type transfer (transfer ratio ↑ 1.0, ↓ 0.1) The transfer properties are dominated by the amylose-acetate (Chapter 2)<sup>2</sup>.

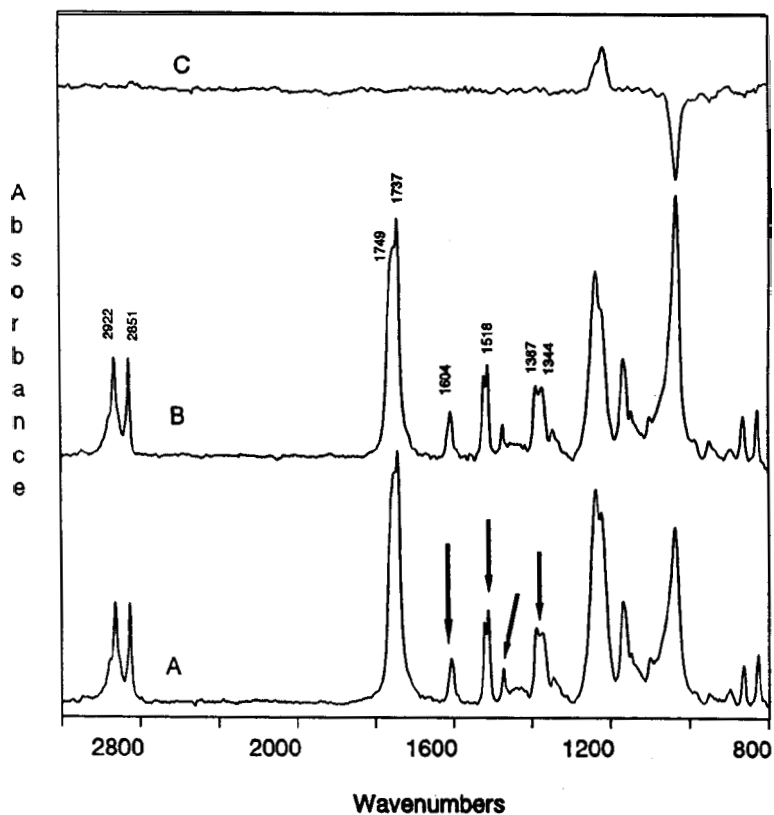


**Figure 4.1** Polarized infrared transmission spectra of a LB-multilayer of mixed monolayers of KMES16/AAC 30/70, 20 layers. A; polarized light perpendicular to the transfer direction. B; polarized light parallel to the transfer direction. C; difference spectrum A-B.

### FT-IR spectroscopy

IR-spectroscopy has the capability to reveal various conformational features and can also be used to determine the orientation of parts of the molecules directly. In this study we used

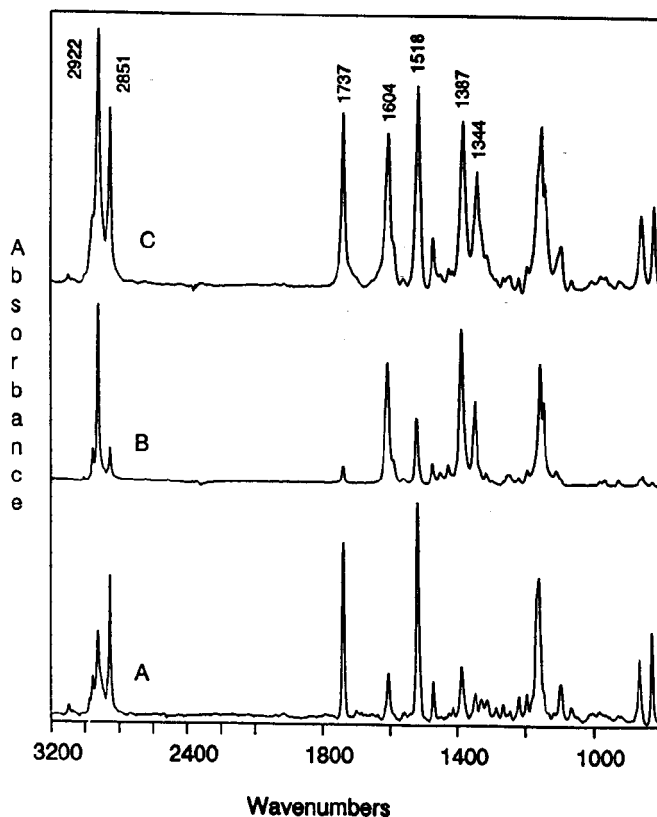
grazing incidence reflection (GIR) spectroscopy and polarized transmission spectroscopy. Samples studied by GIR are deposited on a gold layer on glass. For GIR spectra it is known that individual group vibrations, inducing dipole moment changes of this group, absorb strongly when these dipole moment changes are oriented perpendicular to the reflecting metal mirror. Correspondingly, they will not absorb in the transmission spectra of the same structure, where the electric field vector of the light is parallel to the substrate. Polarized transmission spectroscopy was used to detect orientation effects due to flow induced orientation during the dipping process parallel to the substrate surface. In this experiment **ZnS** was used as the substrate. Details about the used techniques can be found in the literature<sup>8-15</sup>.

Figure 4.1 shows the polarized infrared transmission spectra of 20 layers of a mixed layer (**AAC/KMES16** 70/30) on **ZnS**. Spectrum A was measured with polarization perpendicular to the transfer direction, spectrum B with polarization parallel to the transfer direction. Mode assignments are presented in Table 4.1. The difference of these spectra (A - B) is given in Figure 4.1, curve C. This difference spectrum, representing the orientation in the transfer direction of the multilayers is very similar to the difference spectrum observed in LB-multilayers of pure amylose-acetate<sup>2</sup>. **AAC** forms helices on the water surface which orientate in the transfer direction. The marked absorption bands in Figure 4.1 are due to vibrations of **KMES16** only. The disappearance of these bands demonstrates that the dye molecules are not oriented in the transfer direction. It is important to note that the **AAC** phase behaves independently of the **KMES16** phase.

Figure 4.2 shows the transmission spectrum of 20 layers of **AAC/KMES16** 70/30 (mol%) on **ZnS** (spectrum A) and a GIR spectrum of 9 layers of the same mixture, deposited on a gold substrate is shown in spectrum B. A bulk spectrum of a mixture is given for comparison (spectrum C).

Comparison of the experimental GIR-spectra with transmission spectra should be done with care. GIR-spectra might be distorted compared to transmission spectra<sup>7,15</sup> due to dispersion effects. In order to avoid misinterpretation of spectra, a reflection spectrum of an amorphous film can be calculated in order to have a reference spectrum to compare with the experimental spectrum. This procedure has been described in the literature<sup>15</sup>. In the case of a mixture of a low and high molecular weight compounds the optical constants cannot be derived very accurately. In general, the distortion will be observed mainly at lower frequencies ( $< 1200 \text{ cm}^{-1}$ ) and with strong absorption bands. A reference GIR-spectrum of

amylose-acetate has been calculated before<sup>2</sup> and it turned out that only the C-O-C vibrations around  $1030\text{ cm}^{-1}$  were distorted significantly. Bands below the  $1200\text{ cm}^{-1}$  were not taken into consideration here, so changes in intensity in the GIR- spectrum due to dispersion effects can be neglected.



**Figure 4.2** *Infrared spectra of mixed multilayers of KMES16/AAC 30/70. A; transmission spectrum of 20 layers on ZnS. B; grazing angle reflection spectrum (GIR) of 9 layers on gold. C; bulk spectrum of a mixture, powdered in KBr.*

**Table 4.1** Band assignments

| VIBRATIONS<br>(cm <sup>-1</sup> ) | MODE                          | Transition-<br>moment M                      |
|-----------------------------------|-------------------------------|--|
| 2953                              | $\nu_a$ CH <sub>3</sub>       | $\perp$ C-CH <sub>3</sub>                    |
| 2922                              | $\nu_a$ CH <sub>2</sub>       | $\perp$ C-C-C                                |
| 2851                              | $\nu_s$ CH <sub>2</sub>       | $\parallel$ C-C-C<br>bisecting the HCH angle |
| 1749                              | $\nu$ C=O<br>(amylose-ester)  | $\parallel$ C=O                              |
| 1737                              | $\nu$ C=C<br>(ester KMES16)   | $\parallel$ C=O                              |
| 1604                              | $\nu$ C=C <sub>ar</sub>       | $\parallel$ molecular axis                   |
| 1518                              | $\nu_a$ NO <sub>2</sub>       | $\perp$ molecular axis                       |
| 1472                              | 6 CH <sub>2</sub>             |  |
| 1387                              | $\nu_s$ C <sub>ar</sub> -N    | $\parallel$ molecular axis                   |
| 1344                              | $\nu_s$ NO <sub>2</sub>       | $\parallel$ molecular axis                   |
| 1237                              | C-O-C<br>(coupled motion)     |  |
| 1157                              | C-O-C<br>(ester KMES16)       |  |
| 1146                              | C-O-C<br>(ester KMES16)       |  |
| 1095                              | $\nu_s$ C <sub>aliph</sub> -N |  |
| 1036                              | C-O-C<br>(coupled motion)     |  |
| 864                               | $\nu_s$ C-NO <sub>2</sub>     |  |
| 827                               | 6 1,4 benzene<br>subst.       |  |

A very striking difference between the transmission and GIR-spectra in Figure 4.2 is observed in the area of the CH<sub>2</sub> stretching vibrations (3000 cm<sup>-1</sup> - 2800 cm<sup>-1</sup>). Only



**KMES16** contributes significantly to the absorption bands of the **CH<sub>2</sub>** vibrations. The relative intensities of the bands at **2922 cm<sup>-1</sup>** ( $\nu_a$ ) **CH<sub>2</sub>** and **2851 cm<sup>-1</sup>** ( $\nu_s$ ) **CH<sub>2</sub>** vary remarkably comparing the transmission spectrum to the GIR-spectrum in Figure 4.2.

The intensity of the absorbance of any particular band is given by:

$$I = | \mathbf{M}_i \cdot \mathbf{E} |^2 \approx M_i^2 \cdot \cos^2 \alpha \quad (1)$$

$\mathbf{M}_i$  = dipole transition moment

$\mathbf{E}$  = electrical field

$\alpha$  = angle between  $\mathbf{M}$  and  $\mathbf{E}$

If  $\mathbf{M}_i$  is randomly distributed, the intensity is given by:

$$I \approx c M_i^2 \quad c = \text{constant} \quad (2)$$

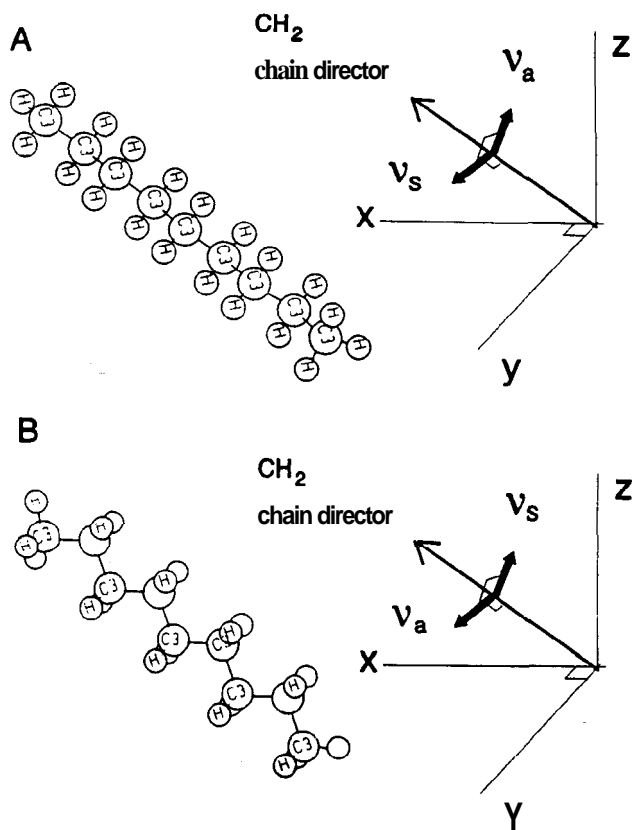
Usually, when the all-trans **CH<sub>2</sub>** chain is oriented at an angle  $\alpha$  with the surface normal,  $\alpha$  can be deduced from observed changes in intensities of the  $\nu_a$  and  $\nu_s$  absorption bands in the transmission mode compared to the GIR mode<sup>10,12</sup>. From the literature<sup>6-15</sup> it is evident that the ratios of the intensities of  $\nu_a$  (**CH<sub>2</sub>**) and  $\nu_s$  (**CH<sub>2</sub>**) do not change significantly. The transition moment of  $\nu_a$  (**CH<sub>2</sub>**) is oriented perpendicular to the transition moment of  $\nu_s$  (**CH<sub>2</sub>**), both in the plane of the **H-C-H** bond. For the all trans alkyl chain the **C-C-C** plane can adapt any orientation around the chain director for one particular  $\alpha$  of the chain director with the surface normal. In that case, the intensity for  $\nu_a$  (**CH<sub>2</sub>**) and  $\nu_s$  (**CH<sub>2</sub>**) depends only on  $M^2$  ( $\nu$ ) and  $M^2$  ( $\nu_s$ ).

Figure 4.2 shows a significant change in the relative intensities of  $\nu_a$  and  $\nu_s$  (**CH<sub>2</sub>**). Table 4.11 lists the relative values of  $\nu_a$  and  $\nu_s$  in the different spectra.

**Table 4.II** *Relative ZR-intensities of the  $\nu_a$  (CH<sub>2</sub>) and  $\nu_s$  (CH<sub>2</sub>) vibrations of LB-layers of mixtures of KMES16 and AAC (30/70). The  $\nu_s$  (CH<sub>2</sub>) band is taken as unity.*

| Spectrum     | $\nu_a$ (CH <sub>2</sub> ) | $\nu_s$ (CH <sub>2</sub> ) |
|--------------|----------------------------|----------------------------|
| Transmission | 1.0                        | 1.0                        |
| GIR          | 5.0                        | 1.0                        |
| Bulk         | 1.4                        | 1.0                        |

Some spectra in the literature <sup>17,18,19,20</sup> showing comparable changes in intensities of  $\nu_a(\text{CH}_2)$  and  $\nu_s(\text{CH}_2)$  have been reported. Nuzzo et al.<sup>19</sup> and Evans et al.<sup>20</sup> explain their results in terms of a close **packing** of the  $\text{CH}_2$  chain in a **triclinic** packing instead of a **orthorombic packing**. The **packing** found by Nuzzo and Evans was induced by strong dipoles of a sulfone group incorporated in the alkyl chain. Here we have a special packed alkyl chain without the incorporation of strong dipole groups in the alkyl chain which can be compared to the model given by Nuzzo<sup>19</sup> and Evans<sup>20</sup>. We suggest that the C-C-C plane does not adapt all possible orientations around the chain director but has a preferred orientation such that this plane is perpendicular to the plane defined by the surface normal and the chain director. This explains the different ratio between  $\nu_s(\text{CH}_2)$  and  $\nu_a(\text{CH}_2)$  bands comparing the transmission spectra to the GIR spectra.



**Figure 4.3** Schematic representation of the two extreme orientations of an all trans aliphatic chain. A represents the suggested structure.

From the spectra in Figure 4.2 it can be deduced that the  $\nu_s$  has a preferred orientation parallel to the film surface because it appears strong in the transmission spectrum and relatively **weak** in the GIR spectrum. The  $\nu_a$  ( $\text{CH}_2$ ) is relative strong in the GIR spectrum compared to the transmission spectra, indicating a large angle ( $\alpha$ ) of the chain director with the surface normal. A schematic representation of the two possible extreme orientations of the **alkyl** chain is presented in Figure 4.3. Figure 4.3(A) represents the suggested situation.

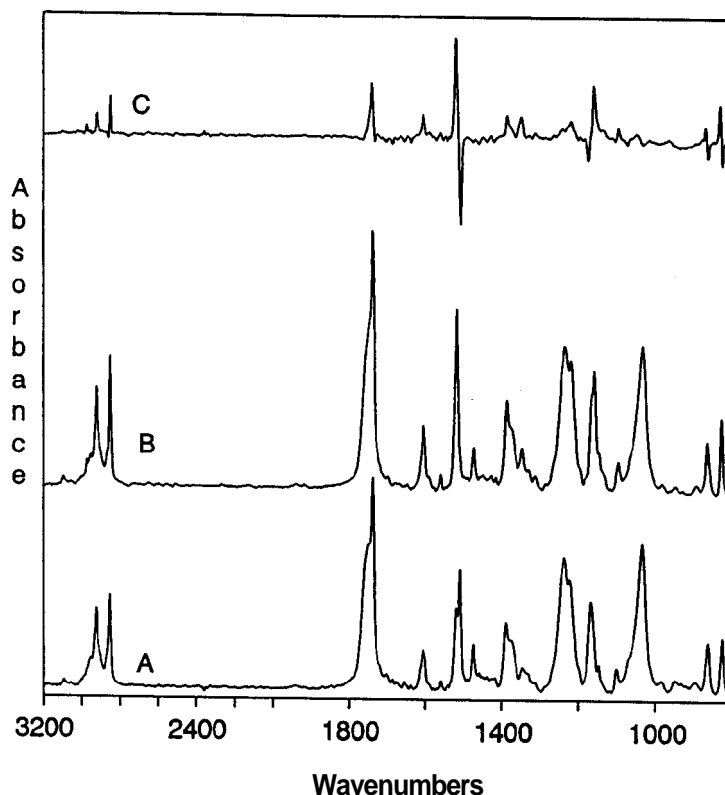


Figure 4.4 Transmission infrared spectra of **LB-multilayers** of KMES16/AAC 30/70. (20 layers) A; as deposited B; after heating to 135 °C and cooling down to room temperature. C; **difference spectrum, B-A.**

The region of  $1800\text{ cm}^{-1}$  -  $1300\text{ cm}^{-1}$  gives information about the orientation of the azo-unit of the dye molecule. The intensity of the vibration bands of  $1604\text{ cm}^{-1}$  and  $1518\text{ cm}^{-1}$  are inverted comparing the GIR-spectrum with the transmission spectrum. This reveals a

preferred orientation of the  $\text{NO}_2$  and azo-benzene groups perpendicular to the surface. Also the increase of intensity of the  $\nu_s \text{C}_{\text{ar}}\text{-N}$  ( $1387 \text{ cm}^{-1}$ ) and  $\nu_s \text{NO}_2$  ( $1344 \text{ cm}^{-1}$ ) in the **GIR**-spectrum compared to the transmission spectrum supports this suggested orientation. The carbonyl region can not be used to obtain specific orientations for one of the components in an accurate way because of the strongly overlapping absorptions of different carbonyls in the mixture.

After heating the LB-multilayer above the melting temperature of the dye ( $129^\circ\text{C}$ ) and cooling down to room temperature the orientation in the multilayers was checked by FT-IR spectroscopy. The result of this experiment is shown in Figure 4.4. Spectrum A corresponds to the LB-film before heating, whereas 4B corresponds to the film after heating. The difference spectrum of these spectra is given in Figure 4.4, spectrum C. All the changes in the spectra after this heating cycle can be explained by a reorganization in the film towards a structure which is even more oriented than before heating. Apparently the sample organizes itself upon cooling again. From the monolayer study<sup>1</sup> of this mixture we know that the dye molecules are packed in crystalline domains. The heating and cooling process of the **multilayer** probably induces an enhanced orientation due to the re-crystallization of the dye domains in the multilayer.

### UV/Visible light spectroscopy.

UV/visible light absorption measurements were carried out in order to obtain more information about the nature of the chromophore unit of the dye molecule. Figure 4.5 shows the UV/visible light absorption spectra with unpolarized light of the dye KMES16 in chloroform (spectrum A). Spectrum B is the absorption spectrum of a LB-layer (**KMES16/AAC 70130**) on one side of a glass slide. The absorption maximum of the dye in solution of chloroform is at 470 nm. The absorption maximum of the dye incorporated in the LB-multilayers shifts to **393 nm**. A shift to lower wavelengths and the observed change in the shape of the absorption band suggests the formation of **H-aggregates**<sup>21</sup>.

In a number of investigations<sup>22,23,24</sup>, the formation of aggregates has been observed. In molecular aggregates exciton effects may be observed when sufficiently strong electronic interaction exist in the molecules<sup>25</sup>. According to this exciton theory strong spectral shifts might appear in the absorption spectra. When only a blue shift is observed it can be argued that the transition moments must be aligned parallel in the aggregates<sup>25</sup>.

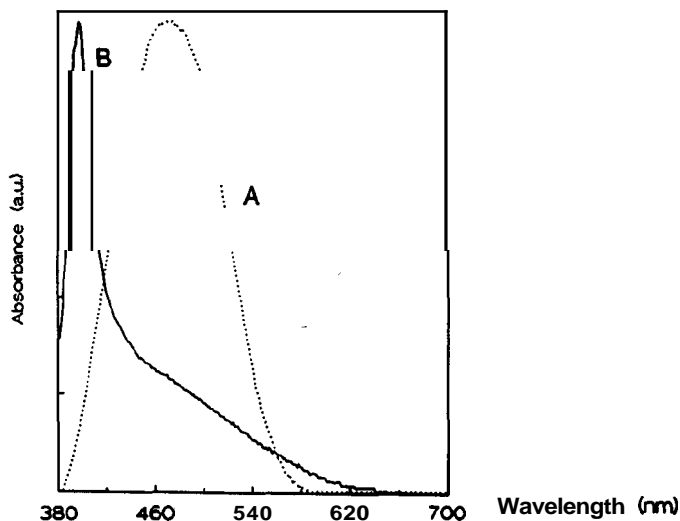
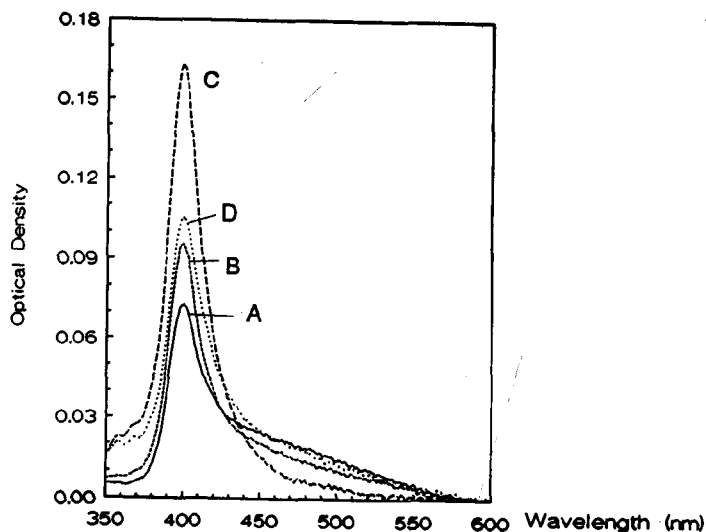


Figure 4.5 UV/Visible light absorption spectra. A; dilute solution of **KMES16** in chloroform. B; LB-multilayer (7l) of **KMES16/AAC 30/70**, as deposited.



**Figure 4.6** Polarized UV/Visible absorption spectra of a multilayer (7l) of **KMES16/AAC 30/70**. A; angle of incidence  $0^\circ$  to the surface normal, polarized light. B; angle of incidence  $30^\circ$  to the surface normal, p polarized light. C; angle of incidence  $60^\circ$  to the surface normal, p polarized light. D; angle of incidence  $60^\circ$  to the surface normal, s polarized light.

Figure 4.6 shows the absorption spectra taken with polarized UV/visible light irradiated at different angles. From these spectra it can be deduced that the chromophore unit of the dye is oriented towards the surface normal at an angle of about  $30^\circ$ . The same qualitative orientation was already found by infrared spectroscopy as described before. The UV/visible light spectra also reveals that a high percentage of the dye is in the aggregated state because the absorbance of the band from non aggregated dye molecules at 470 nm is relatively small at all angles. The nonaggregated dye fraction is also oriented, but in the opposite direction.

#### Small angle X-ray diffraction.

The LB-films of mixtures containing 30 mol%, 50 mol% and 70 mol% **KMES16** give broad X-ray reflections which become sharper when the amount of **KMES16** increases. The mean corresponding spacing of these samples is 32 Å (+2 Å). When the LB-layers are heated above  $129^\circ\text{C}$  and cooled down again, the reflections become much sharper indicating a more regular layer structure. The results are shown in Figure 4.7.

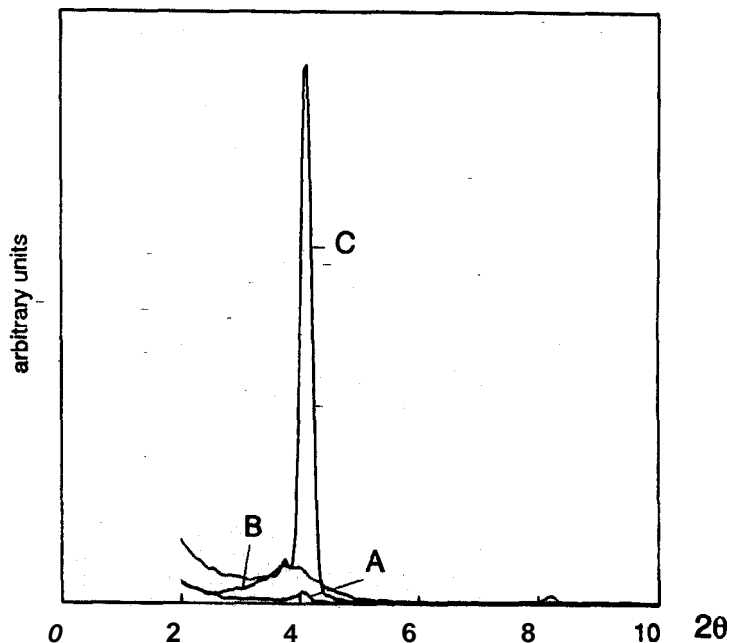
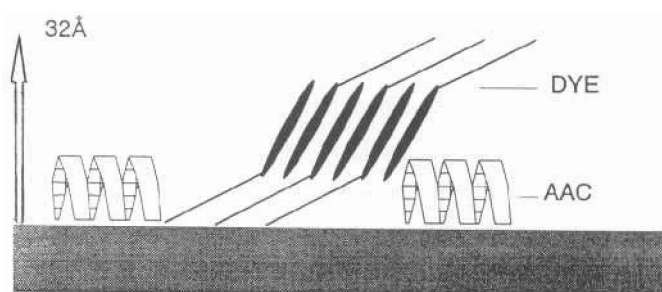


**Figure 4.7** Small angle X-ray diffraction pattern. A; Mixed multilayer, AAC/**KMES16** 30/70, 20 layers. B; Mixed multilayer, AAC/**KMES16** 70/30, 20 layers. C; Mixed multilayer, same as B, after heating to  $135^\circ\text{C}$  and cooling down.

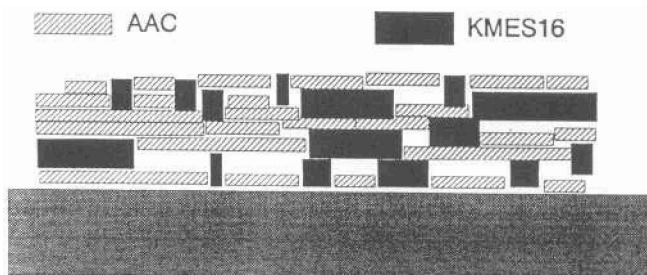
Because the intensity of the X-ray reflection has increased after heating and cooling the layer, the spacing is thought to arise from crystalline domains of the dye. Apparently, recrystallization enhances the layer structure. Multilayers of pure amylose-acetate **do** not exhibit any small angle X-ray reflection peak.

Combining the results of the experimental data leads to the model given in Figure 4.8 for the mixed LB-layers.

Monolayer of KMES16 and AAC.



Multilayer of KMES16 and AAC



Multilayer after heating.

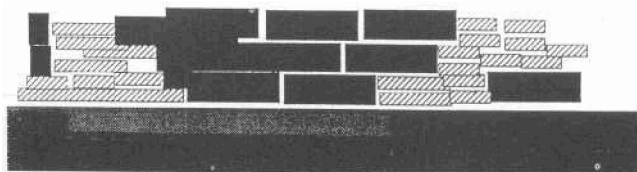


**Figure 4.8** Schematic representation of the suggested model for multilayers of AAC and KMES16.

The **KMES16** is situated in domains and the molecules form H-aggregates. The most convenient orientation of the molecules in the aggregates is an anti-parallel arrangement<sup>1</sup>. The all trans **CH<sub>2</sub>** chains are packed tightly and they have a specific orientation around the chain director. Combining the layer spacing ( $\approx 32\text{\AA}$ ) with the length of the **KMES16** molecule in the extended conformation ( $34.1\text{\AA}$ ) and the orientation for the molecular sub units as revealed by IR-spectroscopy leads to a model with a tilt angle of  $\approx 30^\circ$  to the surface normal for the chromophore unit and a tilt angle of  $60^\circ$  to the surface normal for the **CH<sub>2</sub>** chain. A schematic model of a multilayer is given in Figure 4.8 where the dye molecules are situated in domains. After heating the multilayer reorganizes, resulting in larger dye domains.

## Cast films

### FT-IR spectroscopy.

The orientation of the dye molecule is not a unique feature in the LB-layer of a mixed system. The dye is oriented also in a cast film from a chloroform solution (1mg/ml) onto **ZnS** or gold. Figure 4.9 shows the results. Spectrum A represents a transmission spectrum of a cast film on **ZnS**. Spectrum B shows the GIR spectrum of a cast film onto gold. For comparison the bulk spectrum of **KMES16** is given (Fig.4.9, spectrum C).

The ratio between the  $\nu_a$  (**CH<sub>2</sub>**) absorption band at  $2922\text{ cm}^{-1}$  and  $\nu_s$  (**CH<sub>2</sub>**) at  $2855\text{ cm}^{-1}$  in the **KBr** spectrum of **KMES16** is  $\nu_a : \nu_s = 1.4 : 1.0$ . The layer of the cast film of pure **KMES16** has the values of  $\nu_a : \nu_s = 0.7 : 1.0$ . For the GIR-spectra the following ratio is found:  $\nu_a : \nu_s = 5.1 : 1.0$ . The variation in the observed ratio varies about 5% comparing duplos. The tendency of the observed changes in relative intensities of  $\nu_a$  and  $\nu_s$  in spectra of cast films of **KMES16** coincides with that found in the LB-multilayer of **KMES16/AAC** (30170).

A preferred orientation for the **CH<sub>2</sub>**-chain as is proposed for the **KMES16** domains in a LB-multilayer is also argued for the cast film of pure **KMES16**. The carbonyl band at  $1737\text{ cm}^{-1}$  shows a preferred orientation towards the surface substrate. Comparing to the bulk spectrum of **KMES16**, the  $\nu_s$  (**C=C**) at  $1608\text{ cm}^{-1}$ , the  $\nu_r$  (**C, -N**) at  $1344\text{ cm}^{-1}$  and the  $\nu_a$  (**NO<sub>2</sub>**) have a preferred orientation towards the surface normal. This preferred orientation of the transition dipole moments originate from an orientation of the chromophore unit perpendicular to the



substrate surface.

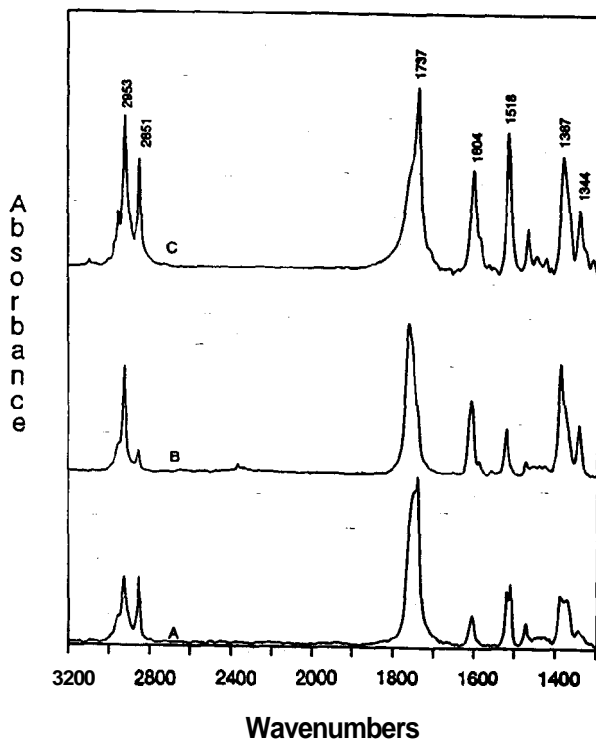


**Figure 4.9** IR-spectra of KMES16. A; cast film on ZnS, transmission mode. B; cast film on gold, GIR mode. C; bulk spectrum of KMES16, powdered in KBr.

#### Small angle X-ray diffraction.

X-ray diffraction measurements of a cast film of KMES16 show a sharp reflection corresponding with a spacing of 32.5 Å. This supports the idea mentioned above that the X-ray reflections arise from the KMES16 domains.

This phenomenon will be studied further in Chapter 5.

## CONCLUSIONS

The mixed monolayers of **KMES16** and AAC can be transferred onto solid substrates . The transfer process is dominated by the properties of the AAC, resulting in Z-type transfer. The **infrared** measurements reveal a specific orientation of the aliphatic chains of the **KMES16** molecules. The aliphatic chains probably have an all trans conformation with the C-C-C chain director at about  $60^\circ$  to the surface normal. A different ratio between  $\nu_s$  ( $\text{CH}_2$ ) and  $\nu_a$  ( $\text{CH}_2$ ) bands comparing the transmission spectrum to the GIR spectrum was found. We suggest that the C-C-C plane does not adapt all possible orientations around the chain director but has a preferred orientation such that this plane is perpendicular to the plane defined by the surface normal and the chain director.

The azobenzene **chromophore** shows a preferred tilt angle of about  $30^\circ$  to the surface normal as revealed by infrared measurements and polarized UV/visible light spectroscopy.

Heating the LB-multilayers above the melting temperature of the dye ( $T_m = 129^\circ\text{C}$ ) and cooling down to room temperature results in an enhanced layer structure in the mixed multilayers. The dye is almost completely in the aggregated state (H-aggregates).

The orientation of the dye molecule is not a unique feature for the LB-multilayers but is also found in cast films of pure **KMES16**.

## REFERENCES

1. Schoondorp, M.A., Schouten, A.J., Hulshof, J.B.E., Feringa, B.L., Oostergetel, G.T.; accepted in *Langmuir* 1992.
2. Schoondorp, M.A., Vorenkamp, E.J., Schouten, A.J. *Thin Solid Films*, 1991, **196**, 121.
3. Feigin, L.A., Lvov, Y.M. *Makromol. Chem. Macromol. Symp.* 1988, 15, . 259.
4. Jark, W., Comelli, G., Russell, T., Stöhr, J. *Thin Solid Fims* 1989, **170**, 309.
5. Teerenstra, M.N., Vorenkamp, E.J., Schouten, A.J., Nolte, R.J.M. *Thin Solid Films* 1991, **196**, 153.
6. Francis, S.A., Ellison, A.H. *J. Opt. Soc. Am.* 1959, 49, 131.
7. Greenler, R.G. *J. Chem. Phys.* 1966, 44, 310,

8. Allara,D.L., Nuzzo,R.G. *Langmuir* 1986, 1, 52.  
Rabolt,J.F., Burns,F.C., Schlotter,N.E., Swalen,J.D., *J. Chem. Phys.* 1983, 78, 946.
10. Chollet,P.A., Messier,J., Rosilio,C.J. *J. Chem. Phys.* 1976, 64, 1042.
11. Duda,G., Schouten,A.J., Arndt,T., Lieser,G., Schmidt,G.F., Bubeck,C., Wegner,G. *Thin Solid Films* 1988, 159, 221.
12. Schneider,J., Ringsdorf,H., Rabolt,J.F. *Macromolecules* 1989, 22, 205.
13. Geddes,N.J., Jurich,M.C., Swalen,J.D., Twieg,R., Rabolt,J.F. *J. Chem. Phys.* 1991, 94, 1603.
14. Arndt,T., Schouten,A.J., Schmidt,G.F., Wegner,G. *Makromol. Chem.* 1991,192,2215.
15. Brinkhuis,R.H.G., Schouten,A.J. *Macromolecules* 1991, 24, 1496.
16. Hulshof,J.B.E., Schudde,E.P., Feringa,B.L., Schoondorp,M.A., Schouten,A.J. to be published.
17. Popovitz-Biro, R., Hill,K., Shavit,E., Hung,D.J., Lahav,M., Leiserowitz,L., Sagiv,J., Hsiung,H., Meredith,G.R., Vanderzeele,H. *J. Am. Chem. Soc.* 1990,112,2498.
18. Gun,J., Iscovici,R., Sagiv.,J. *J. Coll. Interf. Sci.* 1984,101,201
19. Nuzzo,R.G., Fusco,F.A., Allara,D.L. *J. Am. Chem. Soc.*, 1987, 109, 2358.
20. Evans,S.D., Goppert-Berarducci,K.E., Urankar,E., Gerenser,L.J., Ulman,A., Snyder,R.G. *Langmuir*, 1991, 7, 2700.
21. Herz,A.H. *Phorogr.Sci.Eng.* 1974, 18,323.
22. Penner,T.L., Möbius,D., *Thin Solid Films* 1985, 132, 185.
23. Nakahara,H., Möbius,D., *J. Colloid Interface Sci.* 1986, 114, 363.
24. Kawaguchi,T., Iwata,K. *Thin solid films*, 1989, 180, 235.
25. Kasha,M., Rawls,H.R., Ashraf El-Bayoumi,M. In *Molecular Spectroscopy Proc. VIII European Congr. Molec. Spectroscopy*; Butterworth: London, 1965; p371.